

# Crossover between cooperative and fractal relaxation in complex glass-formers

R Golovchak<sup>1</sup>, A Kozdras<sup>2</sup>, O Shpotyuk<sup>3,4</sup> and V Balitska<sup>5</sup>

<sup>1</sup> Department of Physics and Astronomy, Austin Peay State University, Clarksville, TN 37044, USA

<sup>2</sup> Institute of Mathematics and Physics, Opole University of Technology, Opole, PL-45-370, Poland

<sup>3</sup> Institute of Physics of Jan Dlugosz University, Czestochowa, PL-42-200, Poland

<sup>4</sup> Vlokh Institute of Physical Optics, Lviv, UA-79005, Ukraine

<sup>5</sup> Lviv State University of Vital Activity Safety, Lviv, UA-79007, Ukraine

E-mail: [holovchakr@apsu.edu](mailto:holovchakr@apsu.edu)

Received 21 April 2016, revised 14 June 2016

Accepted for publication 15 June 2016

Published 1 July 2016



## Abstract

Kinetics of physical aging at different temperatures is studied *in situ* in arsenic selenide glasses using high-precision differential scanning calorimetry technique. A well-expressed step-like behaviour in the enthalpy recovery kinetics is recorded for low aging temperatures. These fine features disappear when the aging temperature ( $T_a$ ) approaches the glass transition temperature ( $T_g$ ). The overall kinetics is described by stretched exponential function with stretching exponent close to  $3/5$  at  $T_a > \sim 0.95 T_g$  almost independent on glass composition, and  $3/7$  when the aging temperature drops to  $\sim 0.9 T_g$ . These values are consistent with the prediction of Phillips' diffusion-to-traps model. Further decrease in aging temperature to  $\sim 0.85 T_g$  leads to the appearance of step-like behaviour and stretching exponent of  $1/3$  for the overall kinetics, which is the limiting value predicted by random walk on the fractal model. Such behavior is explained as crossover from homogeneous cooperative relaxation of non-percolating structural units to high-dimensional fractal relaxation within hierarchically-arranged two-stage physical aging model.

Keywords: chalcogenide glass, aging, glass transition, structural relaxation

(Some figures may appear in colour only in the online journal)

## 1. Introduction

A vast amount of experimental data suggest that time evolution of the departure from equilibrium of any physical quantity  $\delta(t)$  in disordered electronic and molecular systems obeys Kohlrausch's stretched exponential relaxation rule [1, 2]:

$$\delta(t) = \delta_0 \exp \left\{ - \left( \int_0^t \frac{dt}{\tau} \right)^\beta \right\}, \quad (1)$$

where  $\delta_0$  is the initial departure of physical quantity from equilibrium;  $\tau$  is the effective time constant (the relaxation time); and dimensionless stretching exponent  $\beta$  is a so-called fractional factor (also known as non-exponentiality or dispersivity index),  $0 < \beta \leq 1$  ( $\beta = 1$  for single-exponential relaxation processes and smaller for dispersive processes).

One of the most remarkable examples of such relaxation processes is structural recovery of glasses and polymers (physical aging) [3–6]. Besides the non-exponential character as per equation (1), it is shown also to be a nonlinear in nature, and the nonlinearity is usually accounted by an appropriate model for  $\tau$  determination, assuming that  $\tau$  depends not only on the temperature  $T$ , but also on the instantaneous structure (structural state is usually described by a fictive temperature  $T_F$ ) [1, 7]. The most popular models are the Tool-Narayanaswamy-Moynihan (TNM) [7], Kovacs-Aklonis-Hutchinson-Ramos (KAHR) [8] and Hodge-Scherer [9] ones. All these models, however, do not address the microscopic origin of structural relaxation, describing exceptionally the time behaviour of macroscopic physical quantities (enthalpy losses, volume, stress, strain, refractive index, etc) in a vicinity of glass transition region, and do not accommodate time, temperature or structural dependence of  $\beta$  if present. Despite the

various relaxing properties could be described by different set of model parameters  $\beta$  and  $\tau$ , it looks conceivable that  $\beta$  generally depends on waiting time  $t_w$  below the glass transition temperature (aging duration), degree of nonlinearity of the system and aging/annealing temperature  $T_a$  [1, 2, 9–11]. The evidences for decrease in  $\beta$  with waiting time  $t_w$ , aging temperature and nonlinearity of the system (in the case of thermorheologically complex substances) can be found in some colloidal suspensions and molecular liquids [1, 2, 10, 11], but rarely among glasses.

Most of the experimental and theoretical studies for glasses are performed in the regime near or somewhat below the glass-transition temperature ( $T_a \sim T_g \pm 15\text{--}20\text{K}$ ) [1, 2, 12–15], while a little is known about the structural recovery at well below- $T_g$  temperatures quoted in the literature as *natural physical aging*. Extremely large relaxation times challenge the real-time experiments on capturing a full physical aging kinetics. Frequently, only beginning of the physical aging is recorded and analysed, that causes many discrepancies on the governing kinetics equations (power law, exponential, sum of exponentials or Prony series, stretched exponential, etc) and microstructure mechanisms [6, 15–21].

The most appropriate understanding of structural relaxation relies on heterogeneous scenario of cooperative many-body relaxation processes [1]. According to this, the crossover from independent relaxation (exponential  $\beta$  relaxation with  $\tau \sim \tau_\beta$ ) to heterogeneous cooperative many-body relaxation (stretched exponential  $\alpha$  relaxation with  $\tau \sim \tau_\alpha$ ) was expected in a supercooled liquid regime above  $T_g$  at some time  $t_c$ , introduced by the Coupling Model (which is only one of many competing theories of glass transition), and testified at  $t_c \sim 2\text{ps}$  by neutron scattering experiments [22, 23] and molecular dynamics simulations [24]. Therefore, dynamic heterogeneous nature of structural relaxation extrapolated to the well below  $T_g$  temperatures should be a direct consequence of many-body relaxation dynamics too, and can be viewed as the exchange processes between fast and slow relaxators [1]. It is believed, that there is a correlation between width of the dispersion of structural relaxation ( $\beta$ ) and the length scale of dynamic heterogeneity of the glass-formers ( $\xi$ ), because both are the consequences of many-body relaxation dynamics [1, 25]. A relationship between  $\beta$  and fragility index  $m$  seems to exist too [1, 26, 27], but no direct correlation between length scale of dynamic heterogeneity  $\xi$  and fragility index  $m$  ( $T_g$ -scaled temperature dependence of  $\tau_\alpha$ ) is found so far. Nevertheless, greater  $\xi$  and  $m$  are usually associated with smaller  $\beta$  [1].

There are many instances, however, when the above correlations break down if glass-formers of all kinds are considered all at once [1, 28, 29]. To avoid discrepancies associated with diversity in the nature of glass-formers, the glasses of the same chemical family but different structure should be investigated and compared.

To our opinion, the best model object for such studies is the As–Se family of chalcogenide glasses (ChG). The Se-rich specimens within this system are characterized by relatively fast kinetics of structural relaxation at room temperature in comparison to oxide glasses, for example, that allows studies of almost complete kinetics at accessible

experimental timescales (ranging from a few hours to years) [30, 32] and at broad range of temperatures. On the other hand, by changing chalcogen content in ChG composition it is possible to change the number of mechanical constraints per atom  $n_c$ , which, in turn, affects the length scale of dynamic heterogeneity  $\xi$  and, thus, relaxation behaviour [30]. Structural relaxation in As–Se glasses has been studied recently by differential scanning calorimetry (DSC) as a kinetics of enthalpy losses  $\Delta H(t)$ , over a two decades (20 years) period of natural storage at room temperature [31]. This kinetics is found to have non-elementary character, showing multiple growing steps, the exact number and features of which being not well clear [31, 33, 34]. The multiple step-wise kinetics at well-below- $T_g$  temperatures were assumed to be caused by mixed sequent/parallel hierarchy in the underlying relaxation events, directly dependent on preferential chemical ordering in ChG [34]. The Prony series-like functional was proposed to describe the observed step-wise behaviour of physical aging [33, 34]:

$$\Delta H(t) = \sum_{i=1}^n \theta(t - \Delta t_i) \left[ a_i + b_i \left( 1 - \exp \left( -\frac{t - \Delta t_i}{\tau_i} \right) \right) \right], \quad (2)$$

where  $(t - \Delta t_i)$  is the Heaviside step function;  $\Delta t_i$  is the retardation time giving a time delay between subsequent relaxation steps;  $n$  is the number of steps in the relaxation kinetics;  $a_i$  and  $b_i$  are the weighing factors, which characterize the magnitude of each individual step.

The  $\Delta H(t)$  steps in physical aging kinetics were observed previously for a number of glasses and polymers aged far below  $T_g$  [35–40], but, as a rule, these steps were ignored during the analysis, being attributed to uncertainties in the experimental measurements. Only recently, this behaviour has attracted substantial attention and at least two steps have been unambiguously proved to exist in  $\Delta H(t)$  kinetics of polystyrene (PS) and polycarbonate (PC) polymers [41, 42]. The Brillouin shift measurements in glycerol quenched below  $T_g$  also clearly show step-like behavior, uncovering fast and slow (ultraslow) physical aging dynamics [43]. The number of steps in polymers was assumed to be related to the molecular weight distribution of constituent monomers [34, 41, 42] or relaxation of mechanical strains/tensions [43], but it looks like our understanding of this phenomenon for ChG is still far from being complete.

One of the obstacles is due to the fact that all of the performed long-term physical aging experiments in ChG concerned the enthalpy lost during structural relaxation at room temperature, which was at various distance from  $T_g$  for As–Se glasses with different chalcogen content [31]. It did not allow to elaborate a full picture of structural relaxation in these materials and answer the questions on a reason/criterion to observe the steps/plateaus in the experimental  $\Delta H(t)$  kinetics, as well as their possible number. Therefore, in the present paper we have studied isothermal structural relaxation of As–Se glasses with different backbone connectivity at the aging temperatures  $T_a$ , which were all at the same distance from  $T_g$  for each composition.

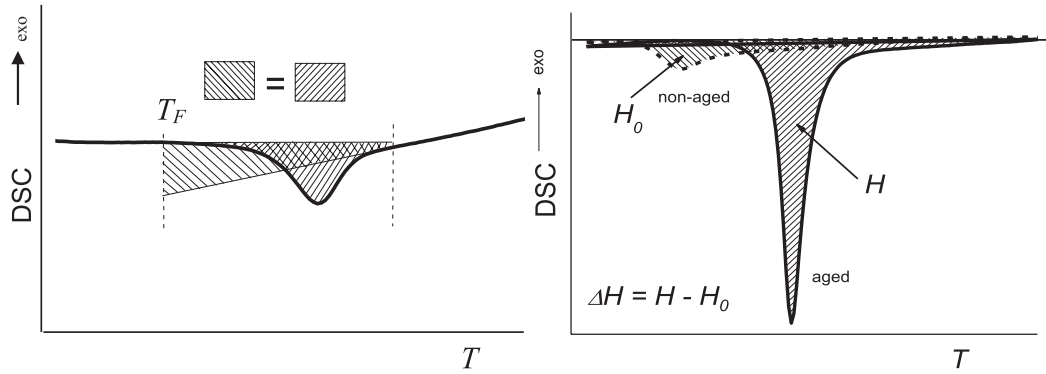


**Figure 1.** Schematic representation of DSC curves, showing Moynihan's graphical method [46] for  $T_F$  determination (left) and method for  $\Delta H$  calculation (right).

## 2. Experiment

The samples of binary  $\text{As}_x\text{Se}_{100-x}$  ( $x = 10, 20, 30, 40$ ) system have been chosen for the investigations. They were prepared by conventional melt-quenching route in the evacuated quartz ampoules from a mixture of high purity (99.999%) As and Se precursors using rocking furnace. All samples were sealed in hermetic plastic bags and stored in the dark at room temperature before the initial calorimetric experiments. Amorphous state of the ChG samples was inspected visually by a characteristic conch-like fracture as well as by x-ray diffraction. Purity and composition of the samples were confirmed by XPS survey and As/Se  $3d$  core level spectra ratios obtained using high-resolution Scienta ESCA-300 spectrometer with monochromatic Al  $K_\alpha$  x-ray (1486.6 eV) as described elsewhere [44].

The DSC measurements were performed in DSC-1 (Mettler Toledo) calorimeter equipped with FRS5+ sensor and IntraCooler accessory. The instrument was calibrated with a set of standard elements: high-purity n-octane, Hg, In and Zn. The DSC curves were acquired in dry nitrogen atmosphere with  $q = 5 \text{ K min}^{-1}$  heating rate. Baseline was subtracted from each DSC signal before the analysis, which was performed using STAR<sup>c</sup> ver. 13a software. The glass transition temperature ( $T_g$ ) was determined as the middle point of glass transition regions according to ISO standard (defined as the intersection point of the bisector of angle and the measurement curve; the angle bisector goes through the intersection point of the baselines before and after transition). Qualitatively similar kinetics are obtained also if  $T_g$  is determined by any other known way (e.g. as onset, peak, inflection or end points). Thus, an example of  $T_g$  onset (determined as cross point of two tangent lines in the beginning of glass-to-supercooled liquid transition region) time dependence is shown in figure 5 for  $\text{As}_{30}\text{Se}_{70}$  sample and compared to the one obtained for middle point. Strictly speaking, none of these  $T_g$  values is a real glass transition temperature, which should be measured in a cooling mode, but rather kind of devitrification (softening) temperature. Nevertheless, it can be used for qualitative discussion along with fictive temperature ( $T_F$ ).

The  $\sim 20 \text{ mg}$  samples were aged *in situ* in the calorimeter, which allowed to reduce the uncertainty associated with human factor as much as possible. The regular rejuvenation procedure

was applied after each cycle to bring the investigated ChG sample into a state close to its initial as-prepared one [45–47]. This procedure comprises heating of the aged sample above its glass transition region, waiting equilibrium at  $T_g + 50 \text{ K}$  and subsequent cooling in a chosen regime at the same cooling rate ( $q = 5 \text{ K min}^{-1}$ ). To verify that the final state of the rejuvenated sample was similar to the initial one (before the aging test), the DSC curves of the rejuvenated samples were compared (they coincided), so the same ChG sample was used to obtain the whole 1 d *in situ*  $\Delta H(t)$  kinetics. *In situ* kinetics were measured twice for each composition and aging temperature, using different samples. The error bars shown on kinetics curves correspond to the maximum uncertainty obtained from statistical and measurements analysis.

## 3. Results

Structural relaxation of polymer glass networks usually results in characteristic endothermic peak superimposed on the endothermic step of experimental heating curves recorded by DSC through the glass-to-supercooled liquid transition (figure 1). It is associated with regaining of the entropy/enthalpy lost during this process. The higher the degree of structural relaxation, the greater the energy loss resulting in larger endothermic peak at  $T_g$  [47]. The difference in the area under this endothermic peak in DSC signal of aged and rejuvenated ChG is directly proportional to the enthalpy losses  $\Delta H$  [30–32, 48]. In fragile glass-formers like Se-rich As–Se glasses, development of the endothermic peak is usually accompanied by  $T_g$  changes (figure 1) [31, 45, 48]. So, recording DSC data for the samples relaxed to a different degree (stored different time at particular conditions) gives the kinetics curves of structural relaxation  $\Delta H(T_a, t)$  and  $T_g(T_a, t)$ , which then can be analysed using various relaxation models. Along with  $\Delta H$  and  $T_g$  values, the fictive temperature  $T_F$  (calculated in present paper according to Moynihan's area method [46]) can also provide a useful information on physical aging, since it describes the instantaneous structural state of a glass [7]. The fictive temperature is known to approach the aging temperature ( $T_a$ ) over a time, which allows to determine unambiguously the degree of physical aging (e.g. the completeness of aging kinetics) [1, 2, 31].

It is shown previously that room temperature ( $T_R$ ) physical aging effects in  $As_xSe_{100-x}$  ChG, associated with slow structural relaxation towards thermodynamic equilibrium of supercooled liquid, are proper to all Se-rich compositions ( $x < 40$ ) up to stoichiometric  $As_{40}Se_{60}$  glass [30, 32], which is supposed to possess an optimally-constrained network in terms of Phillips–Thorpe mean-field rigidity theory [49, 50]. The time dependences of enthalpy losses  $\Delta H(T_R, t)$  at  $T_R \approx 295$  K, determined as the difference between areas under endothermic DSC peaks of aged and rejuvenated  $As_xSe_{100-x}$  ChG (figure 1) [46], exhibited clear plateaus and steep regions (steps) for  $x < 40$  compositions (figure 2(a)), while  $As_{40}Se_{60}$  glass did not age at all during at least ~two decades of storage in a dark at room temperature [31]. Nevertheless, despite a visual perception, the exact number of steps in  $\Delta H(T_R, t)$  kinetics was difficult to determine, because of limited number of experimental points and insufficient accuracy in the *ex situ* DSC measurements. As an example, more frequent and accurate *in situ* measurements reveal few additional steps in  $\Delta H(T_R, t)$  kinetics for  $As_{10}Se_{90}$  glass (figure 3) even during the first day of aging (time-scale of the first step in figure 2(a)). Additionally, as can be inferred from the comparison of  $\Delta H(T_a, t)$  kinetics for  $As_{10}Se_{90}$  glass at  $T_a = 295, 312$  and  $328$  K (figure 2), the steps become less distinguishable when aging temperature increases.

When the investigated samples are brought to the same temperature  $T_a$  in respect to  $T_g$  ( $T_a > 0.8 T_g$ ), all of them exhibited enthalpy losses with time, including also the stable at room temperature  $As_{40}Se_{60}$  glass. Kinetics  $\Delta H(T_a, t)$  curves for 1 d of aging at  $T_a \approx 0.85 T_g$  and  $T_a \approx 0.95 T_g$  are shown in figures 2 and 3 for  $As_{10}Se_{90}$  and in figure 4 for  $As_xSe_{100-x}$  ChG samples with  $x > 10$ . It can be seen, that fine features of  $\Delta H(T_a, t)$  kinetics (plateaus and steep regions) are observed in these glasses (even for stoichiometric  $As_{40}Se_{60}$  glass) on ~day’s timescale at the aging temperature  $T_a \approx 0.85 T_g$ , whereas  $\Delta H(T_a, t)$  curves become smoother with step-like behaviour almost vanished at higher aging temperature  $T_a \approx 0.95 T_g$  (figures 2–4). According to the calculated  $T_F$  data (shown in figures 2–4), the physical aging is fully completed in the case of  $T_a \approx 0.95 T_g$  for all of the investigated ChG, while only part of the kinetics is captured during the first day of aging at  $T_a \approx 0.85 T_g$  (the final  $T_F$  values are far from the aging temperature  $T_a \approx 0.85 T_g$ ). Therefore, it is not conceivable to compare the model parameters ( $\beta$  and  $\tau$ ) for these kinetics, except the  $As_{10}Se_{90}$  glass (figure 2), where  $T_a \approx 0.85 T_g$  coincides with the room temperature  $T_R$  and full kinetics is captured during two decades of natural storage in dark [31].

Different regions can be distinguished in the physical aging kinetics expressed through  $T_g(T_a, t)$  dependences too. At the beginning stage of physical aging, a decrease in  $T_g$  values can be noticed for all ChG compositions (figure 5). It is followed by a region of  $T_g$  increase during longer periods of physical aging, the time constraints for these regions depending essentially on the aging temperature  $T_a$  (figure 5). It is clearly seen, the duration of the first region is about ~400 min in the case of  $T_a \approx 0.85 T_g$ , and decreases to ~30 min at  $T_a \approx 0.95 T_g$ . Dependence on the ChG composition is not so strong, as it

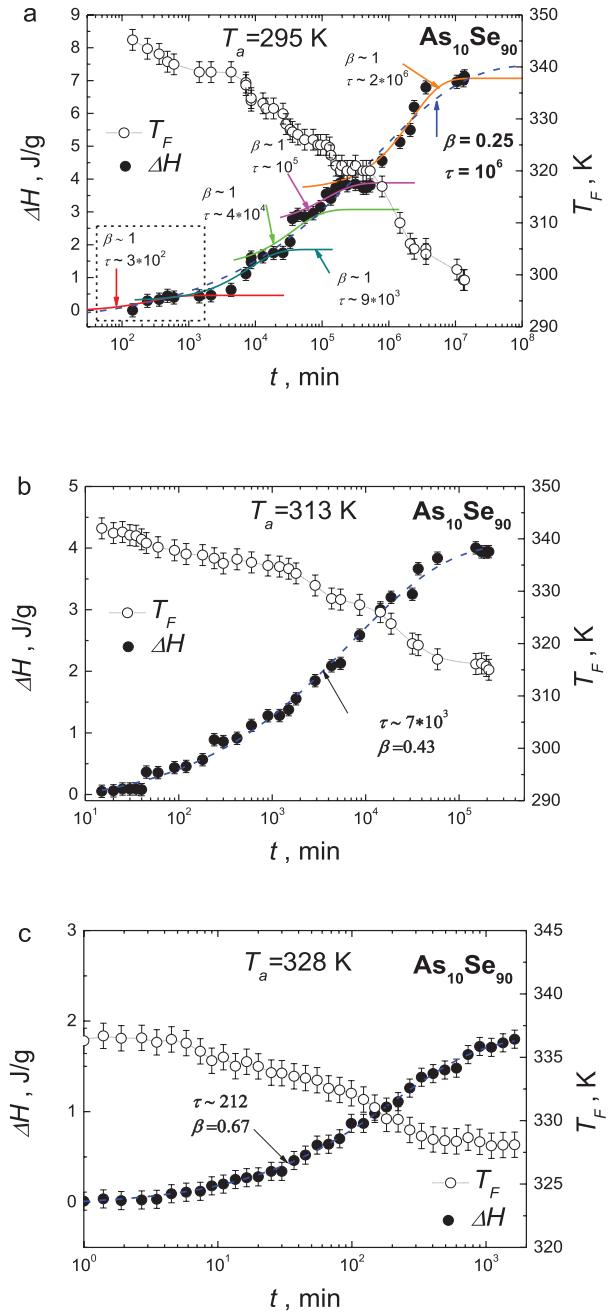


**Figure 2.** Full physical aging kinetics for  $As_{10}Se_{90}$  glass acquired at various temperatures  $T_a = 295$  K (a),  $313$  K (b) and  $328$  K (c). The lines correspond to the fits of overall  $\Delta H(T_a, t)$  curves (dashed lines) and each observed step (solid lines) with equation (1). The parameters of fits  $\beta$  and  $\tau$  (min) are given for each curve.

was assumed previously, when only room temperature kinetics were considered [31]. Although  $T_g$  values obtained from DSC curves in a heating mode according to ISO standard have no significant theoretical importance (real glass transition temperature should be obtained in a cooling mode as vitrification temperature), we have no choice if we want to study physical aging, which is known to be erased when glass is heated above  $T_g$ .

It should be emphasised here again, that the kinetics of physical aging in figures 2(c), 3–5 were measured *in situ*, e.g.

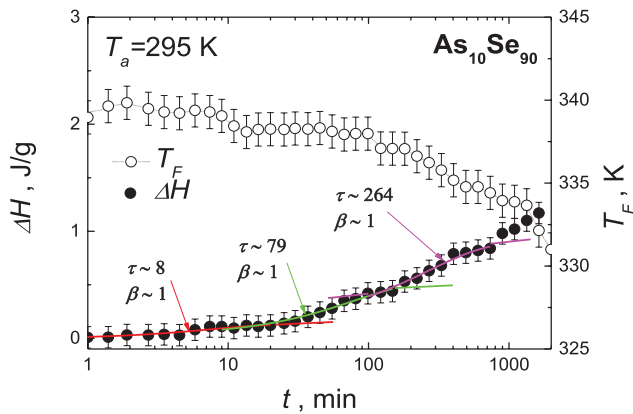


**Figure 3.** Physical aging kinetics for  $\text{As}_{10}\text{Se}_{90}$  glass acquired *in situ* at  $T_a = 295$  K, which corresponds to 1 d interval distinguished by dashed rectangle in figure 2(a). The lines correspond to the fits of the  $\Delta H(T_a, t)$  curve and each observed step with equation (1),  $\tau$  being determined in min.

the DSC curves were precisely recorded for the same carefully prepared sample using similar rejuvenation procedure after each cycle of aging. The experiment was performed directly in DSC calorimeter and the sample was not moved in between the cycles of measurements. So, the observed features should not be considered as artefacts of DSC measuring procedure or human factor, but rather as realistic response of a glass structure to the changes occurred.

#### 4. Discussion

Before the discussion of present results, it is necessary to mention that stretched exponential relaxation function (1) is remarkable in both its accuracy and economy of parameters to describe relaxation kinetics, having only relaxation time  $\tau$  and stretching exponent  $\beta$  as free variables for normalized curves. The universal success of stretched exponential function for many glass-forming systems has led to a conclusion that this type of non-exponential relaxation is structurally intrinsic for microscopically homogeneous disordered media [15]. Therefore, the stretched exponential law was suggested as the main functional form for relaxation behavior of different physical properties in these systems. Specifically, it worked very well for structural relaxation of microscopically homogeneous glasses and polymers in the proximity of  $T_g$  [1–3, 15, 51].

In the present research, the  $\Delta H(T_a, t)$  kinetics curves recorded for  $\text{As}_x\text{Se}_{100-x}$  ChG at  $T_a = 0.95 T_g$  also suggest a stretched exponential form, giving the best accuracy of fit at the cost of minimum free variables. Fitting of these  $\Delta H(T_a, t)$  curves to equation (1) gives  $\beta$  and  $\tau$  parameters as shown in table 1. As it follows from the comparison of data in table 1, the characteristic  $\beta$  values obtained for the investigated glasses from their  $\Delta H(T_a, t)$  kinetics at  $T_a \cong 0.95 T_g$  demonstrate negligible dependence on glass composition, even if some tendency to a slight decrease from  $\beta = 0.67$  for  $\text{As}_{10}\text{Se}_{90}$  glass to  $\beta = 0.62$  for  $\text{As}_{40}\text{Se}_{60}$  glass can be noticed. On the other hand, the length scale of dynamic heterogeneity  $\xi$  is expected

to increase considerably in this compositional trend, which can be ascertained from the peak asymmetry of imaginary part of heat capacity,  $C_p''(T)$ , obtained with temperature modulated DSC [52]. Therefore, a correlation between  $\beta$  and  $\xi$  is barely supported by present studies (at least, through  $\Delta H$  aging kinetics at  $T_a = 0.95 T_g$ ). The same can be ascribed to the correlation between  $\beta$  and fragility index  $m$ , which abruptly drops from 56 to 36 as going from  $\text{As}_{10}\text{Se}_{90}$  to  $\text{As}_{40}\text{Se}_{60}$  composition (table 1) [53]. Contrary to  $\beta$ , the compositional dependence of relaxation time  $\tau$  correlates well with the fragility index  $m$  (table 1) determined at close to  $T_g$  temperatures [53]. If we assume that aging kinetics at  $T_a \cong 0.95 T_g$  is governed by  $\alpha$ -relaxation, then the  $\tau$  values in table 1 can be directly associated with  $\alpha$ -relaxation time constants  $\tau_\alpha$ , since the fragility index is nothing else but  $T_g$ -scaled temperature dependence of this parameter [2].

Nevertheless, a nice sigmoidal shape of  $\Delta H(T_a, t)$  curves ceases, when physical aging occurs at well below  $T_g$  temperatures. From comparison of  $\Delta H(T_a, t)$  kinetics recorded at  $T_a \cong 0.85 T_g$  and  $T_a \cong 0.95 T_g$  (figures 2 and 4), it is clear that plateaus and steep regions appear, when aging temperature  $T_a$  departs more from  $T_g$ . It was shown previously that such kind of behaviour could be accurately described by a sum of simple exponentials, like equation (2), originating from sequence of relaxation processes [31, 33]. Although at the first look such an approach leads to increased number of free variables in fitting (statistical weight and time constant for each single exponent), which is an obvious disadvantage over a stretched exponential function (1) with only 2 free variables, it converges into stretched exponential-like behavior if hierarchical scheme of approaching the equilibrium is considered [54]. The latter means that atoms, or groups of atoms, might only be able to move appreciably when several of the fastest atomic motions happen in just the right way, leaving a hole or weakening a bond. This is exactly what is happening during two stages of physical aging mechanism proposed earlier [31, 55]. The faster degrees of freedom successively constraining the slower ones, seems to be the only reasonable way of generating a wide range of relaxation times. So, to make a connection between glass structure and existence of plateaus and steep regions in  $\Delta H(T_a, t)$  dependence well below  $T_g$ , it is necessary to consider current state of the atomistic mechanism describing physical aging in ChG.

Structural data obtained earlier for a number of Se-rich As–Se glasses suggest that physical aging below  $T_g$  is based on elementary relaxation acts of inner Se atoms within double-well potentials (DWP) associated with high flexibility of chalcogen bonds [52, 55]. These twisting motions of individual Se atoms within DWP (can be associated with *cis-trans* re-conformations of Se atoms in longer Se chains, for example) result in the appearance of collapsed (aligned) regions in a glass network and, consequently, local free volumes around these collapsed regions (well confirmed by direct *in situ* measurements with positron annihilation lifetime spectroscopy) [56]. Such perturbations should be accompanied also by the appearance of elastic strains in the immediate surroundings of collapsed regions [57]. We believe these changes are most significant in virgin (non-aged) glasses, they being responsible

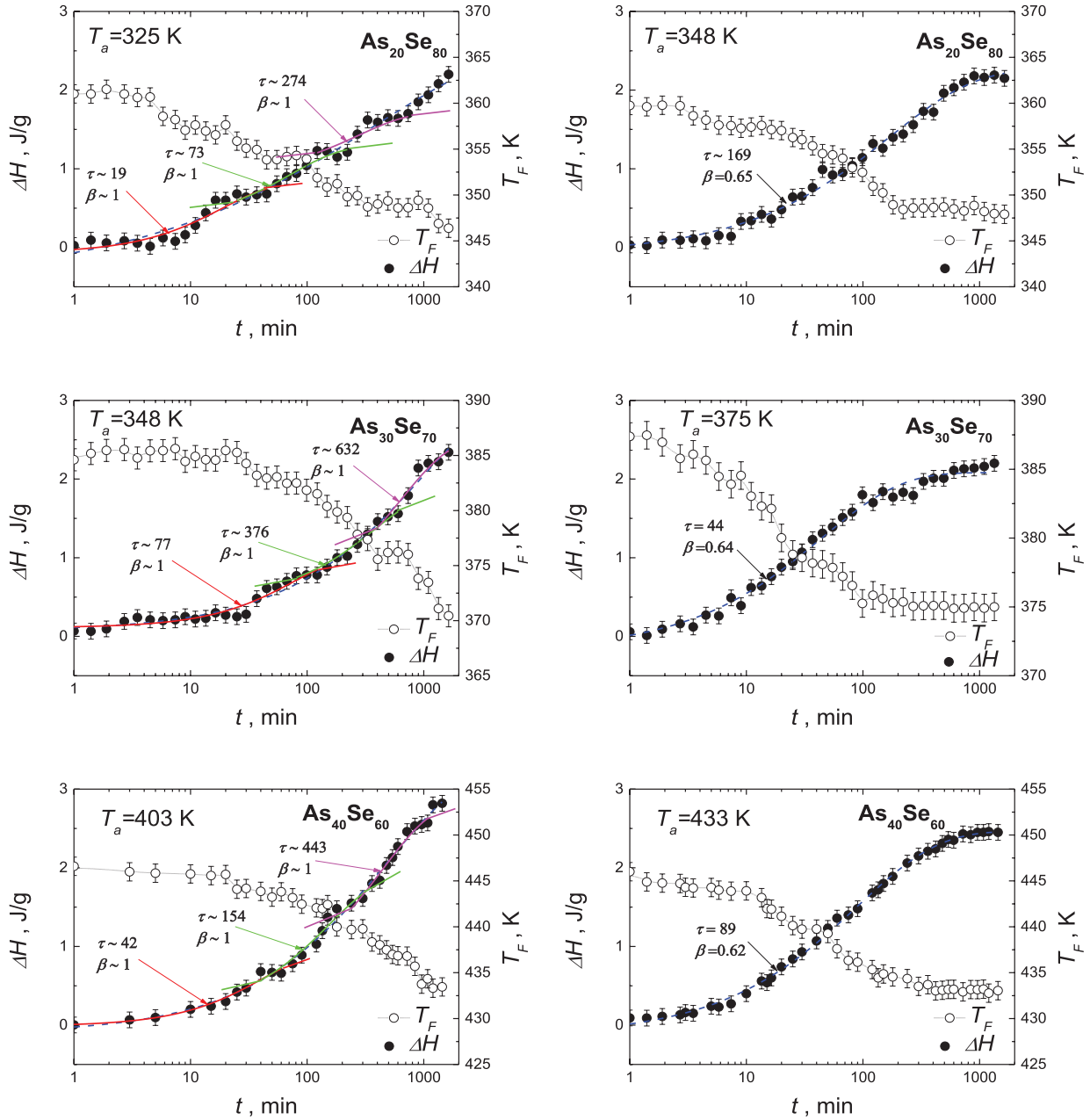


**Figure 4.** Physical aging kinetics for  $As_{20}Se_{80}$ ,  $As_{30}Se_{70}$  and  $As_{40}Se_{60}$  ChG acquired at  $T_a \cong 0.85 T_g$  (left panel) and  $T_a \cong 0.95 T_g$  (right panel) aging temperatures *in situ*. The lines correspond to the fits of overall  $\Delta H(T_a, t)$  curves (dashed lines) and each observed step (solid lines) with equation (1). The parameters of fits  $\beta$  and  $\tau$  (min) are shown for each case.

for  $T_g$  lowering during the initial stage of physical aging (figure 5). The reasons for this  $T_g$  reduction can be similar to the mechanisms proposed for the same in thin films as compared to bulk polymers [58]. In particular,  $T_g$  depression in PS films was explained by enhanced segmental dynamics, chain architecture and presence of mechanical stresses [59, 60]. Moreover, in thin polymer films the increased recovery rate of equilibrium (taken as a slope of the recovery function) was observed and confirmed by molecular dynamics simulations [61, 62]. If we accept that main structural difference between thin film and corresponding bulk glass consists in the amount of free volume (thin amorphous films usually are characterized by a larger content of free volume available for

relaxation), the appearance of additional free volume in bulk ChG during physical aging should increase the recovery rate towards the equilibrium too. This is indeed observed as steep regions in  $\Delta H(T_a, t)$  aging kinetics at much lower than  $T_g$  temperatures (figures 2 and 4). During the second stage of physical aging, it is believed that cooperative rearrangements occur eliminating the redundant free volume from the glass, which lowers the potential energy of the system, or, that is the same, transfers the system to lower metabasin on potential energy landscape [63]. Therefore, this stage of physical aging yields general shrinkage (densification) of ChG network, which can be described, for example, within free volume hole diffusion models [64].

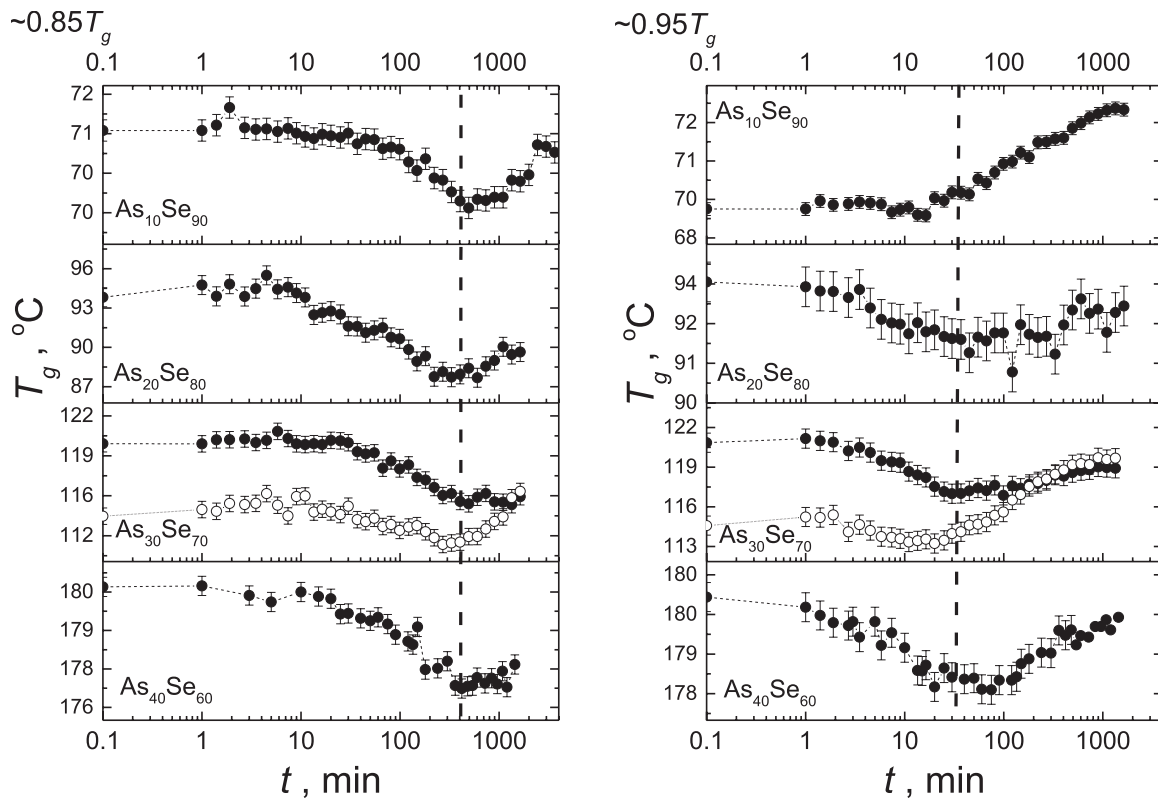


**Figure 5.** Dependence of the glass transition temperature  $T_g$  (midpoint—full symbols, onset—open symbols) on time during physical aging of  $\text{As}_{10}\text{Se}_{90}$ ,  $\text{As}_{20}\text{Se}_{80}$ ,  $\text{As}_{30}\text{Se}_{70}$  and  $\text{As}_{40}\text{Se}_{60}$  glasses at  $T_a \cong 0.85 T_g$  (left panel) and  $T_a \cong 0.95 T_g$  (right panel) temperatures.

**Table 1.** Fitting parameters of physical aging kinetics  $\Delta H(T_a, t)$  shown in figures 2–4.

ChG sample	$T_a \cong 0.95 T_g$ (1 d aging)				$T_a \cong 0.85 T_g$ (1 d aging)			$T_a = T_R$ (~20 years aging)		
	$T_a, K$	$\beta (\pm 0.05)$	$\tau, \text{min}$ ( $\pm 5$ )	$m$	$T_a, K$	$\beta (\pm 0.05)$	$\tau, \text{min}$ ( $\pm 10$ )	$\beta (\pm 0.05)$	$\tau, \text{min}$ ( $\pm 10\%$ )	$T_a/T_g$
$\text{As}_{10}\text{Se}_{90}$	328	0.67	213	56	295	0.70	1464	0.25	$\sim 10^6$	0.85
$\text{As}_{20}\text{Se}_{80}$	348	0.65	169	34	325	0.57	220	0.28	$\sim 10^7$	0.80
$\text{As}_{30}\text{Se}_{70}$	375	0.64	44	31	348	0.62	981	0.35	$\sim 10^9$	0.75
$\text{As}_{40}\text{Se}_{60}$	433	0.62	89	36	403	0.61	488	n/a	n/a	0.65

*Note:* The parameters for ~20 years kinetics at room temperature ( $T_R$ ) are taken from [31] and the fragility indexes  $m$  from [53]. Italic font means that only partial kinetics was fitted with (1) and the obtained parameters of fit have no strict physical meaning.

The above mechanism has to be activated in multiple cycles in order to explain numerous plateaus and steep regions in the observed  $\Delta H(T_a, t)$  kinetics (figures 2–4). Each cycle should involve more and more extended atomic rearrangements, in harmony with a well-known fact that size of cooperative rearranging region (CRR) increases with aging [65]. This increase in CRR size means entanglement of chains in high molecular weight polymers [66]. In ChG this process can be imagined as a formation and sequential growth of the fractals, defined as internally non-relaxing structural entities formed by collapsed regions and/or relaxed/rigid structural units. These fractals grow/percolate with aging duration, thus explaining the gradual increase in the relaxation times  $\tau$  of the Prony-like series in equation (2). Indeed, the off-equilibrium (non-multifractal) decay is known to be faster than quasi-equilibrium decay of grown topological tree (local multifractal domain) [67]. Of course, the size and dimensionality of the fractals and,

therefore, the magnitude and number of steps in the aging kinetics would depend on the amount of rigid structural units sturdy to relaxation, which, in turn, is determined by the number of constraints per atom. The more constraints per atom we have, the larger fractals are expected in a glass due to percolation of rigid structural units. The number of constraints is known to be temperature dependent, e.g. the constraints become active/inactive, when the temperature drops/rises below/above a certain value [68]. Therefore, it is naturally that increase in  $T_a$  causes temperature degeneracy of some constraints, which restricts the size and, possibly, the dimensionality of fractals, ultimately leading to a homogeneous  $\alpha$ -relaxation (Johari–Goldstein relaxation) scenario [1] described by stretched exponential behaviour (1). We believe there exists a *crossover* between the high-dimensional fractal relaxation and homogeneous cooperative relaxation of non-percolating structural units (could be approached by low-dimensional fractals dynamics).

Indeed, one could notice in table 1 that  $\beta$  values fitted for the physical ageing kinetics at  $T_a \cong 0.95 T_g$  are remarkably close to  $\beta = 3/5$ , one of the two ‘magic’ numbers predicted by axiomatic diffusion-to-traps model of Phillips [15, 69]. According to this model, the stretching exponent can be calculated as  $\beta = fd/(fd + 2)$ , where  $d$  is the dimension of Cartesian scattering space and  $f$  is the fraction of channels activated for the particular relaxation process [15]. It approaches  $\beta = 3/5$  in 3D space, provided all available channels are equally activated for relaxation ( $f = 1$ ) [15]. The stretched exponential relaxation can be directly emerged from the diffusion-to-traps model using simple topological considerations, not involving fractal approach [14]. If we further speculate that relaxational channels are associated with possible chemical environments for Se atoms (like, for example, Se–Se–Se or Se–Se–As in  $\text{As}_{10}\text{Se}_{90}$  glass) [44] and corresponding DWPs, then activation/deactivation of these channels would depend if the thermal energy associated with aging temperature is enough to overcome the corresponding energetic barrier between two wells or not, which is equivalent to removing/placing some angular constraints on Se atom. In turn, relaxation of such ‘pure’ structural units can be complicated by the overlap of differently relaxing structural fragments, which can form additional relaxational channels. For example, if Se–Se–Se and Se–Se–As fragments physically overlap (as in the case of short Se chains like =As–Se–Se–Se–As=), they can form relaxational channel in addition to those associated with each of these two environments, increasing the total number of possible channels. In such a way we can obtain a broad spectrum of  $\beta$  values. If we increase the total number of channels up to 4 (as in the case, for example, when unrelaxed Se–Se–Se and Se–Se–As fragments form two channels, and structural agglomerations based on previously relaxed Se–Se–Se and Se–Se–As sites form another two channels, which can further relax with greater relaxation times as low-dimensional fractals), the set of possible values for  $\beta$  would be 0.27, 0.43, 0.53 and 0.6 for  $f = 1/4, 2/4, 3/4$  or  $4/4$ , respectively; to 5—we would have  $\beta = 0.23, 0.375, 0.47, 0.545$  and 0.6 according to the Phillips’ field-free diffusion-to-traps model [15], and so on. It is likely that there would be a superposition of different processes in structurally complicated ChG networks, leading to deviations from pure minimalist diffusion-to-traps model. Therefore, it is not a surprise that  $\beta$  values for a variety of ChG were reported to be near  $\sim 0.5$  [70, 71], although Moynihan, Eastaer *et al* reported the  $\beta$  value of  $2/3$  for  $\text{As}_{40}\text{Se}_{60}$  glass based on the enthalpy relaxation at  $T_a = 420$  K [12, 72], which is in good agreement with  $\beta = 0.62$  obtained in our experiment at  $T_a = 433$  K (figure 4, table 1).

If the aging temperature drops well below  $T_g$ , the hierarchical scheme of approaching the equilibrium should be considered and high-dimensional fractal nature of relaxation prevails. This results in a step-like behaviour of  $\Delta H(T_a, t)$  physical aging kinetics, which is shown to be adequately described by Prony-like series (2). However, the overall kinetics can still be well fitted with stretched exponential

function (1), if steps are ignored, as shown in table 1 for  $\text{As}_{10}\text{Se}_{90}$  and  $\text{As}_{20}\text{Se}_{80}$  ChG aged for more than  $\sim 2$  decades at room temperature (full physical aging kinetics is captured). The fractional exponent  $\beta$  in this case is close to  $1/3$  (table 1), which is the limiting value obtained for percolating fractals of  $n \geq 6$  dimensions within the random walk on fractals model [73]. According to this model, the percolating fractals are considered as  $n$ -dimensional hyperspheres in  $(n + 1)$ -embedding dimensional space, on which surface  $\sigma$ -size structural units percolate. The stretching exponent  $\beta$  depends not only on the dimensionality of the fractal ( $n$ ), but also on the diameter  $\sigma$  of percolating units (hyperdisks in the original work [73]). The latter could be a key for understanding a weak compositional dependence of  $\beta$  for physical aging at  $T_a \cong 0.95 T_g$  (table 1). Thus, alternatively to Phillips’ diffusion-to-traps model [15, 69], the value of stretching exponent  $\beta = 0.67$  for physical aging of  $\text{As}_{10}\text{Se}_{90}$  glass at  $T_a \cong 0.95 T_g$  (table 1) can be explained within random walk on fractals model considering low-dimensional ( $n = 3$ ) percolating cluster, built of structural units with  $\sigma \sim 0.20$  (arb. u.) diameter [73]. The  $\beta$  value of 0.62 character for structural relaxation of glassy  $\text{As}_{40}\text{Se}_{60}$  at  $T_a \cong 0.95 T_g$  (table 1) would also correspond to percolating cluster of  $n = 3$  dimension, but made of  $\sigma \sim 0.14$  (arb. u.) diameter units [73]. The structural origin of these percolating units, however, remains an open question. As an interesting challenge for further numerical simulations would be a striking correlation between the ratio of  $\sigma$  diameters for  $\text{As}_{10}\text{Se}_{90}$  and  $\text{As}_{40}\text{Se}_{60}$  glasses ( $0.20/0.14 \approx 1.4$ ) with the ratio of CRR linear dimensions as determined from temperature-modulated DSC [74]. This correlation probably justify a simple additive principle of forming percolating clusters built on relaxed/unrelaxed Se–Se–Se, Se–Se–As, As–Se–As structural fragments, governing physical aging kinetics in these ChG. The observed decrease in the  $\beta$  value to  $1/3$  with decrease in the aging temperature  $T_a$  allows us to assume the increase in fractal dimensionality  $n$  and, probably, fractal’s average size, invoking random walk on fractals model [73].

The existence of crossover between cooperative and fractal relaxation (smooth and step-like behaviour) can explain many peculiarities and discrepancies in structural relaxation kinetics. For example, dramatic deviations from the extrapolated liquid-like behaviour (when glass system reaches limiting  $T_F$  different from  $T_a$ ), observed in some glassy polymers at  $T_a \ll T_g$  [17], can be explained by termination of the experiment when a first noticeable plateau in  $\Delta H(T_a, t)$  dependence is reached. Existence of plateaus in  $\Delta H(T_a, t)$  kinetics can also explain the partial enthalpy recovery after short-term physical aging at  $T_a < T_g$ , observed, for example, in  $\text{Ge}_x\text{Se}_{100-x}$  glasses [75]. Smooth structural relaxation kinetics, which are usually used as arguments for non-diverging dynamics in glass-forming polymers [76], could be explained by a proximity of  $T_a$  to  $T_g$ , and so on. The exact crossover temperature, however, would depend on the origin of thermodynamic system and, as a result, can be different for different glass-formers.

## 5. Conclusions

It is conceivable from the present results that fine features in  $\Delta H(T_a, t)$  physical aging kinetics become more frequent and decrease in amplitude, when  $T_a$  approaches  $T_g$ , which results in smooth kinetics curves merging into single stretched exponential relaxation behaviour. At close to  $T_g$  temperatures, all relaxation channels occur to be equally activated, which leads to stretching exponent  $\beta$  of 3/5 predicted by Phillips' diffusion-to-traps model. With decrease in the aging temperature, the Phillips' diffusion-to-traps model can still be applied under an assumption that only part of relaxation channels is active. As an example, the stretching exponent  $\beta$  approaches the value of 3/7 in  $\text{As}_{10}\text{Se}_{90}$  glass aged at  $T_a = 313$  K, predicted by Phillips diffusion-to-traps model for half of the relaxation channels being active. Further decrease in the aging temperature leads to the entanglement of different structural units, the most probably, due to the activation of additional constraints, that leads to prevailing of high-dimensional fractal dynamics in the physical aging kinetics with limiting stretching exponent  $\beta$  close to 1/3 as predicted by random walk on fractals model. We suggest that multiple plateaus and steep regions in  $\Delta H(T_a, t)$  aging kinetics are caused by hierarchical scheme of approaching the equilibrium, when faster degrees of freedom successively constrain the slower ones. This scheme corresponds to fractal approach and agrees well with two-stage physical aging mechanism proposed earlier. If the number of constraints approaches the space dimensionality (3 for structural covalent glasses under consideration), the fractals grow enormously, blocking all possible relaxation channels at laboratory timescale as in the case of  $\text{As}_{40}\text{Se}_{60}$  glass stored at room temperature.

## Acknowledgment

R Golovchak thanks to NSF Grant DMR-1409160.

## References

- [1] Ngai K L 2011 *Relaxation and Diffusion in Complex Systems* (Berlin: Springer)
- [2] Angell C A, Ngai K L, McKenna G B, McMillan P F and Martin S W 2000 *J. Appl. Phys.* **88** 3113
- [3] Struik L C E 1978 *Physical Aging in Amorphous Polymers and Other Materials* (Amsterdam: Elsevier)
- [4] Kurchan J 2005 *Nature* **433** 222
- [5] Hutchinson J M 1995 *Prog. Polym. Sci.* **20** 703
- [6] Nemilov S V 2000 *Glass Phys. Chem.* **26** 511
- [7] Narayanaswamy O S 1971 *J. Am. Ceram. Soc.* **54** 491
- [8] Kovacs A J, Aklonis J J, Hutchinson J M and Ramos A R 1979 *Polym. Sci. Polym. Phys. Ed.* **17** 1097
- [9] Hodge I M 1991 *J. Non-Cryst. Solids* **131–3** 435
- [10] Stickel F 1995 *Untersuchung der dynamik in niedermolekularen flüssigkeiten mit dielektrischer spektroskopie* (Aachen: Shaker)
- [11] Di-Leonardo R, Gentilini S, Ianni F and Ruocco G 2006 *J. Non-Cryst. Solids* **352** 4928
- [12] Moynihan C T et al 1976 *Ann. New York Acad. Sci.* **279** 15
- [13] Simon S L, Plazek D J, Sobieski J W and McGregor E T 1997 *J. Polym. Sci. B* **35** 929
- [14] Potuzak M, Welch R C and Mauro J C 2011 *J. Chem. Phys.* **135** 214502
- [15] Phillips J C 1996 *Rep. Prog. Phys.* **59** 1133
- [16] Nemilov S V 2001 *Glass Phys. Chem.* **27** 214
- [17] Messeguer Duenas J M, Vidaurre Garayo A, Romero Colomer F, Mas Estelles J, Gomez Ribelles J-L and Monleon Pradas M 1997 *J. Polym. Sci. B* **35** 2201
- [18] Klafter J and Shlesingert M F 1986 *Proc. Natl Acad. Sci. USA* **83** 848
- [19] Koontz E, Blouin V, Wachtel P, Musgraves J D and Richardson K 2012 *J. Phys. Chem. A* **116** 12198
- [20] Khamzin A A, Popov I I and Nigmatullin R R 2013 *J. Chem. Phys.* **138** 244502
- [21] Chen K and Schweizer K S 2007 *Phys. Rev. Lett.* **98** 167802
- [22] Colmenero J, Arbe A, Goddens G, Frick B, Mijangos C and Reinecke H 1997 *Phys. Rev. Lett.* **78** 1928
- [23] Colmenero J, Alegria A, Arbe A and Frick B 1992 *Phys. Rev. Lett.* **69** 478
- [24] Affouard F, Cochon E, Danede F, Decressain R and Descamps M 2005 *J. Chem. Phys.* **123** 084501
- [25] Qiu X H and Ediger M D 2003 *J. Phys. Chem. B* **107** 459
- [26] Plazek D J and Ngai K L 1991 *Macromolecules* **24** 1222
- [27] Bohmer R and Angell C A 1992 *Phys. Rev. B* **45** 10091
- [28] Shahriari S, Mandanici A, Wang L-M and Richert R 2004 *J. Chem. Phys.* **121** 8960
- [29] Ngai K L 2005 *Phys. Rev. B* **71** 214201
- [30] Golovchak R, Jain H, Shpotyuk O, Kozdras A, Saiter A and Saiter J-M 2008 *Phys. Rev. B* **78** 014202
- [31] Golovchak R, Kozdras A, Balitska V and Shpotyuk O 2012 *J. Phys.: Condens. Matter* **24** 505106
- [32] Golovchak R, Kozdras A, Shpotyuk O, Kozyukhin S and Saiter J-M 2009 *J. Mater. Sci.* **44** 3962
- [33] Balitska V, Golovchak R, Kozdras A and Shpotyuk O 2014 *Physica B* **434** 21
- [34] Shpotyuk O, Kozdras A, Balitska V and Golovchak R 2016 *J. Non-Cryst. Solids* **437** 1
- [35] Alves N M, Manoa J F and Ribelles J L G 2001 *Polymer* **42** 4173
- [36] Lixon Buquet C, Hamonic F, Saiter A, Dargent E, Langevin D and Nguyen Q T 2010 *Thermochim. Acta* **509** 18
- [37] Barral L, Cano J, Lopez J, Lopez-Bueno I, Nogueira P, Abad M J and Ramirez C 1999 *Eur. Polym. J.* **35** 403
- [38] Qu T 2004 Non-aging and self-organization in network glasses *PhD Thesis* Faculty of Electrical Engineering, University of Cincinnati
- [39] Andreozzi L, Faetti M, Giordano M and Zulli F 2005 *Macromolecules* **38** 6056
- [40] Boucher V M, Cangialosi D, Alegria A and Colmenero J 2011 *Macromolecules* **44** 8333
- [41] Cangialosi D, Boucher V M, Alegria A and Colmenero J 2013 *Phys. Rev. Lett.* **111** 095701
- [42] Cangialosi D 2014 *J. Phys.: Condens. Matter* **26** 153101
- [43] Miller R S and MacPhail R A 1997 *J. Chem. Phys.* **106** 3393
- [44] Golovchak R, Kovalskiy A, Miller A C, Jain H and Shpotyuk O 2007 *Phys. Rev. B* **76** 125208
- [45] Saiter J M, Arnoult M and Grenet J 2005 *Physica B* **355** 370
- [46] Moynihan C T, Eastal A J and Wilder J 1974 *J. Phys. Chem.* **78** 2673
- [47] Utz M, Debenedetti P G and Stillinger F H 2000 *Phys. Rev. Lett.* **84** 1471
- [48] Shpotyuk O, Golovchak R and Kozdras A 2014 Physical aging of chalcogenide glasses *Chalcogenide Glasses: Preparation,*

- Properties and Application (Woodhead Publishing Series in Electronic and Optical Materials vol 44)* ed J-L Adam and X Zhang (Cambridge: Woodhead) pp 209–64
- [49] Phillips J C 1979 *J. Non-Cryst. Solids* **34** 153
- [50] Thorpe M F 1983 *J. Non-Cryst. Solids* **57** 355
- [51] Welch R C et al 2013 *Phys. Rev. Lett.* **110** 265901
- [52] Golovchak R, Oelgoetz J, Vlcek M, Esposito A, Saiter A, Saiter J-M and Jain H 2014 *J. Chem. Phys.* **140** 054505
- [53] Yang G, Gulbiten O, Gueguen Y, Bureau B, Sangleboeuf J-C, Roiland C, King E A and Lucas P 2012 *Phys. Rev. B* **85** 144107
- [54] Palmer R G, Stein D L, Abrahams E and Anderson P W 1984 *Phys. Rev. Lett.* **53** 958
- [55] Golovchak R, Shpotyuk O, Kozdras A, Bureau B, Vlcek M, Ganjoo A and Jain H 2007 *Phil. Mag.* **87** 4323
- [56] Golovchak R, Ingram A, Kozdras A, Vlcek M, Roiland C, Bureau B and Shpotyuk O 2012 *Phil. Mag.* **92** 4182
- [57] Nemilov S V and Johari G P 2003 *Phil. Mag.* **83** 3117
- [58] Cangialosi D, Alegria A and Colmenero J 2016 *Prog. Polym. Sci.* **54-5** 128
- [59] Fakhraai Z and Forrest J A 2005 *Phys. Rev. Lett.* **95** 025701
- [60] Gao S, Koh Y P and Simon S L 2013 *Macromolecules* **46** 62–570
- [61] Priestley R D, Ellison C J, Broadbelt L J and Torkelson J M 2005 *Science* **309** 456
- [62] Tang Q, Hu W and Napolitano S 2014 *Phys. Rev. Lett.* **112** 148306
- [63] Mauro J C and Smedskjaer M M 2012 *Physica A* **391** 3446
- [64] Cangialosi D, Curro J G, Lagasse R R and Simha R 1982 *Macromolecules* **15** 1621
- [65] Donth E 2001 *The Glass Transition Relaxation Dynamics in Liquids and Disordered Materials (Materials Science)* (Berlin: Springer)
- [66] Bouthegourd E, Esposito A, Lourdin D, Saiter A and Saiter J-M 2013 *Physica B* **425** 83
- [67] Yoshino H 1997 *J. Phys. A: Math. Gen.* **30** 1143
- [68] Smedskjaer M M, Mauro J C, Sen S and Yue Y 2010 *Chem. Mater.* **22** 5358
- [69] Macdonald J R and Phillips J C 2005 *J. Chem. Phys.* **122** 074510
- [70] Rekhson S M and Ginzburg V A 1976 *Sov. J. Glass Phys. Chem.* **2** 422
- [71] Shieh S H M and LaCourse W C 1993 *Mater. Chem. Phys.* **35** 160
- [72] Easteal A J, Wilder J A, Mohr R K and Moynihan C T 1977 *J. Am. Ceram. Soc.* **60** 134
- [73] Jund P, Jullien R and Campbell I 2001 *Phys. Rev. E* **63** 036131
- [74] Saiter A, Saiter J-M, Golovchak R, Shpotyuk M and Shpotyuk O 2009 *J. Phys.: Condens. Matter* **21** 075105
- [75] Zhao H Y, Koh Y P, Pyda M, Sen S and Simon S L 2013 *J. Non-Cryst. Solids* **368** 63
- [76] McKenna G B and Zhao J 2015 *J. Non-Cryst. Solids* **407** 3